
The Regularizing Effect of Different Output Layer Designs in Deep Neural Networks

Anonymous Author(s)

Affiliation

Address

email

Abstract

1 Deep neural networks are prone to overfitting, especially on small datasets. Com-
2 mon regularizers such as dropout or dropconnect reduce overfitting, but are complex
3 and prone to hyperparameter choices, thus prolonging development cycles in prac-
4 tice. In this paper, we propose simple but effective design changes to the output
5 layer - namely randomization, sparsity, activation scaling, and ensembling - that
6 lead to improved regularization. These designs are motivated by experiments
7 showing that standard fully-connected output layers tend to rely on individual
8 input neurons, which in turn do not cover the variance of the data. We call these
9 two related phenomena *neuron dependency* and *expressivity*, propose different
10 ways to measure them, and optimize the presented output layers for them. In our
11 experiments, we compare these layer types for image classification and semantic
12 segmentation across architectures, datasets, and application settings. We report sig-
13 nificantly and consistently improved performance of up to 10% points in accuracy
14 over standard output layers while reducing the number of trainable parameters by
15 up to 90%. It is demonstrated that neither training of output layers is required, nor
16 are output layers themselves crucial components of deep networks.

17 1 Introduction

18 Neural networks are powerful feature extractors that have become the standard approach for a myriad
19 of tasks. New architectures are continuously introduced and set records on benchmark datasets
20 (e.g. [24, 15, 44]). These networks differ in layer composition, depth/width or use specific concepts
21 such as residual connections [15] or self-attention [34]. With growing capacity, their performance on
22 large datasets tends to increase [44]. However, model complexity is also associated with overfitting,
23 especially for small datasets where fine details of the training data are easily memorized [52, 2, 53].

24 Rather than defining another, possibly more complex architecture, we analyze what often remains
25 unconsidered: the output layer. In image classification, networks usually end with a fully-connected
26 (fc) layer that combines extracted features for the final output [43, 15, 17, 44]. As we will show, this
27 layer is prone to overfitting since high dependencies on individual, possibly memorized features can
28 arise. The same neurons are subsequently not able to generalize across examples. We call these two
29 related phenomena *neuron dependency* and *expressivity* and illustrate a simplified example in Fig. 2.

30 Both problems can be improved by simple but effective changes to the output layer that require only
31 few lines of code and achieve better generalization (i.e., better results on the test set [25], see e.g.
32 Fig. 1). Those changes rely on four principles: activation scaling, fixed randomization, sparsity and
33 in-layer ensembling (see Fig. 5). This work analyzes all layers in terms of their capability to reduce
34 dependencies and/or increase expressivity. Then, the connection to network performance is shown
35 through a comprehensive empirical study across datasets, architectures and application settings in
36 image classification and segmentation. Furthermore, we investigate how stronger regularization

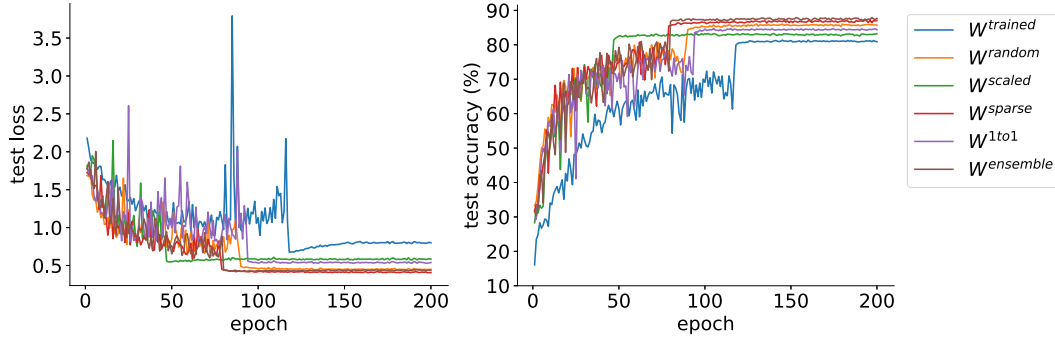


Figure 1: Effect of different output layer designs on cross-entropy loss (**left**) and accuracy (**right**) in a ResNet-50 for the STL-10 dataset. Best viewed in color.

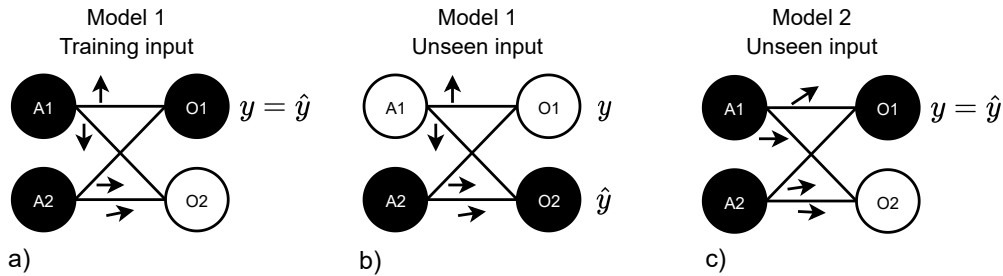


Figure 2: Schematic of neuron dependency/expressivity in fc output layers. The left side of each subfigure represents penultimate layer activations (A1-2), the right shows output neurons for each class (O1-2). Filled/blank circles indicate high/low activation, up-/downward facing arrows signal positive/negative weights. Higher activations of O1 lead to correct predictions in this example. Model 1 depends on neuron A1 to be activated to give high prediction scores to O1. This is the case for a training instance in **a**). If Model 1 is applied to an unseen input pattern of same class in **b**), higher scores are erroneously given to O2 since A1 remains inactive and A2 slightly favors O2. Model 1 fails to generalize as it depends on A1, which is not expressive enough to cover the variance of the target class. Instead, Model 2 shown in **c**) exhibits neurons with low dependency and high expressivity, where A1 generalizes to unseen patterns, while the activation of A2 can be regarded as backup. Note that this example is simplified and educational. See Sect. 3.3 for measurements.

37 can be induced by applying the identified principles to other parts of a network while reducing the
 38 computational footprint. In contrast to common practice, we find neither training of output layers
 39 to be necessary, nor that output layers are crucial components of deep networks. In summary, our
 40 **contributions** are:

- 41 • Introducing neuron dependency and expressivity as two factors contributing to overfitting
 42 and proposing ways to measure these factors
- 43 • Showing improved regularization of 5 different output layer designs up to 10% in absolute
 44 accuracy compared to standard fc layers and other common regularizers
- 45 • Empirical results showing that the proposed layers have improved dependency and expressiv-
 46 ity, computational efficiency, wide applicability to both small and large datasets, extensibility
 47 to other parts of the network, and robustness in the choice of hyperparameters

48 2 Related Work

49 Regularization in deep learning is approached in various ways. Widely used methods are, e.g.,
 50 normalization [19, 3], weight decay [32], data and adversarial augmentation [40, 1], early stopping [7],
 51 boosting [38], multitask learning [6], dropout [42], dropconnect [50], and Gaussian noise layers [10].
 52 To the best of our knowledge, this is the first work that evaluates regularization with respect to

53 different output layer designs. Similar to dropout/dropconnect, output layers can be categorized as
 54 affecting the architecture according to the regularization taxonomy described in [25]. Unlike other
 55 regularizers, our methods are either hyperparameter-free or robust to their choice and can be applied
 56 to any deep net, including pre-trained ones that are less affected by overfitting (see Sect. 5.4 and 5.7).

57 Related to fixed randomization are the output layers used in [16, 39, 14], which show comparable
 58 performance to trained layers. One can also preallocate output layer weights with a defined struc-
 59 ture [31, 16]. Besides output layers, weight fixing is for example applied to the first layer in the
 60 Extreme Learning Machine [18], or to different weight dimensions in [36]. In contrast, we omit
 61 hand-crafted weights, show improved regularization and relate to neuron dependencies. Further, we
 62 show that fixing or scaling the last conv block next to the output layer has a strong regularizing effect.

63 Sparsity is common in deep learning, e.g. the ReLU activation [13] or a L_1 penalty term in the loss
 64 function [46]. Sparsity has also been applied to the channels of Convolutional Neural Networks
 65 (CNNs) [8, 29]. Others induce sparsity by pruning connections before training under the lottery
 66 ticket hypothesis [11, 30], with the goal of reducing the number of parameters while not sacrificing
 67 performance [27, 45, 51]. Different to them, we show that (extreme) sparsity is not merely useful to
 68 improve computational efficiency, but to improve performance when applied to the output layer.

69 The Network in Network (NIN) [28] and All-CNN [41] both use global average pooling (GAP)
 70 followed by softmax, which replaces the fc output layer with an identify transform to simplify the
 71 network. This is further analyzed in [33]. We show its connection to neuron dependency/expressivity
 72 and achieve comparable or better performance on various datasets. Further, we observe that previous
 73 works do not leverage the full capacity of the last layer in modern networks, which enables the
 74 construction of computationally efficient in-layer ensembles that further boost performance in small
 75 and large datasets.

76 3 Neuron dependency and expressivity

77 3.1 Setting and notation

78 We consider neural networks consisting of an encoder $f_{enc} : \mathbf{X} \rightarrow \mathbf{a}$ followed by an output layer
 79 $f_{out} : \mathbf{a} \rightarrow \hat{\mathbf{y}}$. In this paper, the encoder is a CNN, taking as input an image $\mathbf{X} \in \mathbb{R}^{C \times H \times W}$ with
 80 C , W and H being input channels, width and height, respectively; and transforming it to a feature
 81 vector $\mathbf{a} \in \mathbb{R}^{1 \times N}$. Commonly in CNNs, 2D representations resulting from the final conv layer
 82 are aggregated by GAP [28] where N corresponds to the number of pooled conv channels. The
 83 output layer transforms the embedding to output $\hat{\mathbf{y}} \in \mathbb{R}^K$ holding the probabilities of K classes.
 84 The output layer is parameterized by a weight matrix $\mathbf{W} \in \mathbb{R}^{N \times K}$, and is commonly initialized as
 85 $\mathbf{W}^{random} \sim \mathcal{U}(-\sqrt{1/N}, \sqrt{1/N})$ [26]. Both $\hat{\mathbf{y}}$ and target \mathbf{y} are used to compute the cross-entropy
 86 loss $\ell = -\sum_i^K y_i \log(\hat{y}_i)$. We use the terms features/channels/nodes or neurons interchangeably
 87 meaning activations \mathbf{a} . When required, we refer to individual instances with a superscript, e.g.
 88 $(\mathbf{X}^{(i)}, \mathbf{y}^{(i)}) \in \mathcal{D}$, with \mathcal{D} being a dataset. Corresponding subsets are denoted as \mathcal{D}_{train} and \mathcal{D}_{test} .

89 3.2 Concepts

90 During training, CNNs learn a set of visual patterns that are combined for a classification decision.
 91 However, if patterns remain undetected, e.g. due to noise in the image or inherent but unseen variance
 92 in the data, their activation values can become small and thus reduce the output values for the target
 93 class. When a network is overfitting, it learns malignant image-specific patterns by heart [52]. Such a
 94 network may depend on the activation of individual nodes, which in turn fail to generalize to patterns
 95 that are salient to a class. We call these two related phenomena neuron dependency and expressivity.

96
 97 **Neuron dependency:** How much does a model depend on a single neuron? In a network
 98 with high neuron dependencies, output scores and thus performance drop significantly when certain
 99 neurons remain inactive. In contrast, a network with low neuron dependencies distributes activations
 100 across many neurons, so that a single inactive node does not have much influence on the classification.

101 **Neuron expressivity:** How much class-specific variance does a neuron cover? Neurons with low
 102 expressivity focus on unimportant details that do not characterize the properties of a class. In contrast,
 103 a neuron with high expressivity generalizes by activating to various patterns pertinent to a given class.

104 An example of neuron dependency/expressivity for a simplified fc output layer is illustrated in Fig. 2.

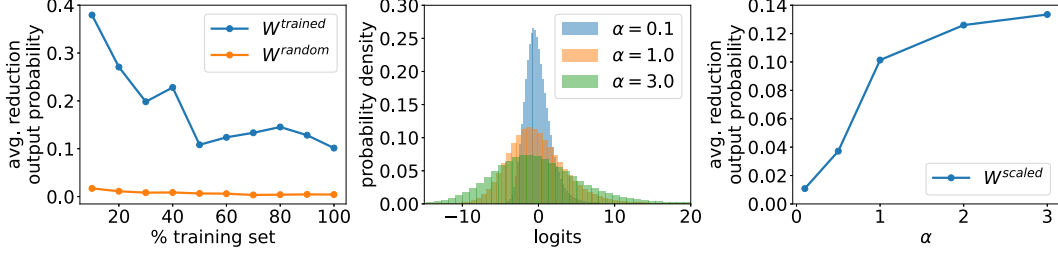


Figure 3: The effect of dataset size and activation scale on neuron dependency in a ResNet-50 trained on subsets of **CIFAR-100**, evaluated on the test set. **Left**: Small training sets lead to high neuron dependencies. **Center**: Scaling activations results in larger absolute logits. **Right**: Larger scales lead to higher dependencies. Best viewed in color.

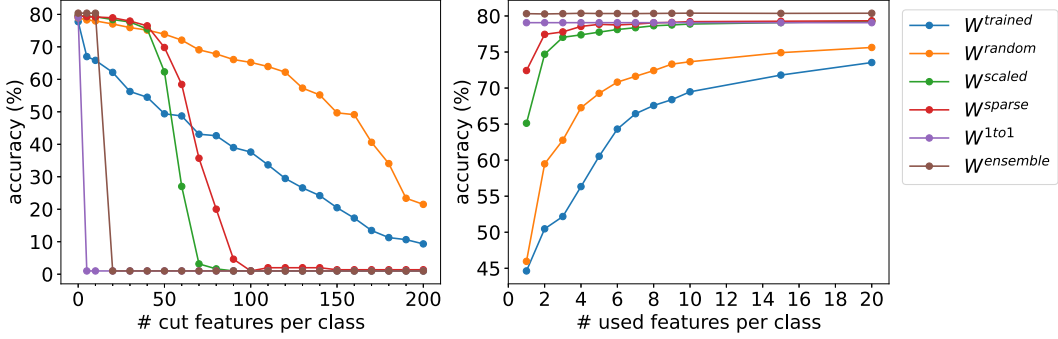


Figure 4: Neuron dependency (**left**) and expressivity (**right**) in a ResNet-50 with 2048 penultimate layer channels trained on **CIFAR-100** for different output layer designs, showing the change in accuracy on the test set. Best viewed in color.

105 **3.3 Measuring dependency and expressivity**

106 We introduce two ways of measuring dependency/expressivity: instance-based and class-based. The
 107 former is used to determine the dependency on the most important node for the predicted class given an
 108 instance. Importance scores for node n and output class \hat{k} are computed with Gradient \odot Activation [4],
 109 a global attribution method where we leverage the partial derivative of the softmax values:

$$a_n \frac{\partial \hat{y}_{\hat{k}}}{\partial a_n}. \tag{1}$$

110 Instance-based dependency is then measured as avg. reduction in output probabilities when ablating
 111 the most important feature w.r.t. the output class of any instance. This is illustrated for various
 112 training set sizes of CIFAR-100 [23] in Fig. 3 (left). With less data, fc output layers tend to depend
 113 more on single nodes. This is in contrast to class-based measures, which enable quantifying both
 114 dependency/expressivity and use various features jointly. Importances are determined for each class
 115 k and over all test instances:

$$\sum_{i=1}^{|\mathcal{D}_{test}|} a_n^{(i)} \frac{\partial \hat{y}_k^{(i)}}{\partial a_n^{(i)}}. \tag{2}$$

116 Class-based dependency is then measured as drop in accuracy when ablating a given number of most
 117 important neurons per class. Measuring expressivity reverses this - the most important neurons per
 118 class are retained, all others are ablated. This is illustrated for both dependency/expressivity in Fig. 4.
 119 We see that standard (i.e. trained) fc output layers tend to depend on single channels to achieve high
 120 performance, but these very channels hold only limited class information.

121 **4 Output Layer Types**

122 We describe several simple output layer variants that require minimal changes to standard networks,
 123 decrease neuron dependency and/or increase neuron expressivity. All types are illustrated in Fig. 5.

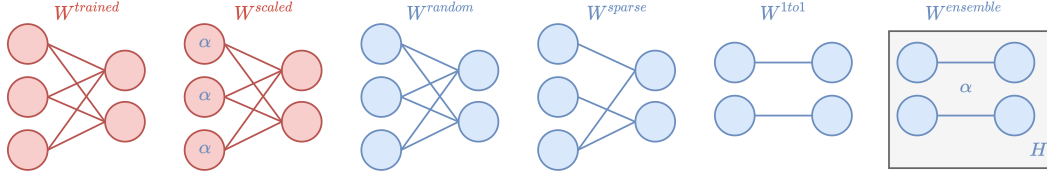


Figure 5: A visual comparison of various output layer types. Red/blue represent variable/fixed.

124 4.1 Standard output layers

125 The ubiquitous approach to compute class scores is to learn the parameters of a weight matrix
 126 $\mathbf{W}^{trained}$, s.t. $\hat{\mathbf{y}} = \sigma_{SM}(\mathbf{a}\mathbf{W}^{trained})$ with $\sigma_{SM}(\cdot)$ being softmax. Each feature is considered in the
 127 computation of each class score. As shown in Sect. 3, trained fc output layers can lead to high neuron
 128 dependencies, where the deletion of a single neuron might cause significant loss in performance, and
 129 low neuron expressivity, where multiple features are required for adequate predictions.

130 4.2 Scaled output layers

131 The reduction of an activation, e.g. due to changing light conditions, has a large influence on the
 132 output scores. This is simulated in Fig. 3 (center) by multiplying features during training with a
 133 scalar $\alpha > 0$, so that $\hat{\mathbf{y}} = \sigma_{SM}(\alpha\mathbf{a}\mathbf{W}^{scaled})$. Note that the variances of the output logit distributions
 134 increase with α , resulting in larger differences (or smaller entropies) after softmax normalization.
 135 This results in greater dependencies of the model on individual neurons, as shown in Fig. 3 (right).
 136 However, if α is chosen small, the activations of individual neurons become insufficient for class
 137 discrimination with high confidence. The model is therefore forced to learn multiple class-specific
 138 features for each instance, which increases the expressivity of the neurons and also reduces their
 139 dependencies to some extent, as shown in Fig. 4. If not specified otherwise, we use $\alpha = 0.1$.

140 4.3 Random fixed layers

141 This setting uses \mathbf{W}^{random} during training/inference, and its classification performance was first
 142 analyzed in [16]. The encoder learns to extract patterns that adjust to predetermined weights. Unlike
 143 activation scaling, the parameters are bounded and fixed to a small value range. For any class, the
 144 chosen uniform initialization is expected to assign similar weight values to multiple neurons, making
 145 them learn similar features. We suppose that the enforced similarity reduces dependency shown in
 146 Fig. 3 and 4 (both left), while small initialization values increase expressivity as in Sect. 4.2, shown
 147 in Fig. 4 (right).

148 4.4 Sparse fixed layers

149 In sparse output layers, class nodes use predetermined sets of channels, some of which might
 150 be shared across classes. First, a set of cutting indices \mathcal{I}_k is randomly sampled for each class
 151 k , where sparsity is determined by the proportion q of class-specific connections to cut, so that
 152 $|\mathcal{I}_k| = \lfloor qN \rfloor$ with $0 < q < 1$. Then, starting from a fixed random initialization as in Sect. 4.3, weights
 153 connecting to a given class are ablated so that: $\mathbf{W}_{i,k}^{sparse} = 0 \forall i \in \mathcal{I}_k$. Hyperparameter q trades
 154 off dependency/expressivity. Larger values induce more sparsity, leading to greater dependencies to
 155 the remaining nodes, but forcing them to activate across instances, making them expressive. We set
 156 $q = 0.9$ in the experiments to show that high sparsity benefits generalization.

157 4.5 1-to-1 correspondence layers

158 The most extreme type of sparsity in an output layer is one with a single connection between a
 159 feature and a class. If these connections correspond to an identity transform, the activations of the
 160 penultimate layer are equivalent to the class logits - in practice, the output layer can hence be omitted.
 161 This was analyzed in [33, 28] and showed comparable results to a standard output layer. Formally, we
 162 have $\hat{\mathbf{y}} = \sigma_{SM}(\mathbf{a}\mathbf{W}^{1to1})$ with $\mathbf{a} \in \mathbb{R}^{1 \times K}$ and $\mathbf{W}^{1to1} \in \mathbb{R}^{K \times K}$, where $\mathbf{W}^{1to1} = \text{diag}(1, 1, \dots, 1)$.
 163 In this layer, both the model's dependency on individual neurons as well as each neuron's expressivity
 164 are maximal. If a single neuron is ablated, the output logits for the class this neuron is connected to is

165 reduced to zero. However, individual neurons learn to cover the whole variance of a given class in the
166 training set, which is one conjecture for their performance. Note that as mentioned in [33], we have
167 the constraint $N = K$, which might be restrictive for small networks and large numbers of classes.

168 4.6 Ensemble layers

169 Is there a way to optimize for both low neuron dependency and high expressivity? Of the approaches
170 discussed, 1-to-1 correspondence layers have the highest expressivity. Starting from this layer, a
171 simple approach to reduce neuron dependency is to use the capacity of the penultimate layer and
172 create multiple heads $h = 1 \dots H$ with $N = KH$, each head being a 1-to-1 correspondence layer.
173 Each head’s output is effectively computed as $\hat{\mathbf{y}}^h = \sigma_{SM}(\alpha \mathbf{a}^h)$ with \mathbf{a}^h being the activation part of
174 head h . As in Sect 4.2, we introduce a scalar α , which controls the magnitude of feature activations.
175 For consistency, we denote this approach as \mathbf{W}^{heads} . The loss is computed for each head and
176 averaged: $\frac{1}{H} \sum_{h=1}^H \ell(\hat{\mathbf{y}}^h, \mathbf{y})$. Similarly, logits are averaged over heads for inference. Due to the
177 induced redundancy, the performance only drops considerably after removing class-related neurons
178 from all heads. In our experiments, we set H to its maximum given any setting (architecture/dataset).
179 Note that hyperparameter α in ensemble layers is the only one which is tuned to individual settings.

180 5 Experiments

181 We aim to show that the presented output layers from Sect. 4 outperform standard output layers and
182 common regularization methods in various settings. Details about training, compute resources, code,
183 datasets as well as additional experiments on dependency/expressivity are included in the appendix.

184 5.1 Small-scale and fine-grained classification

185 All layer types are first applied to small-scale and/or fine-grained classification, both of which are
186 challenging and require regularization. Datasets include STL-10 (500 img/class) [9], CUB-200 (~30
187 img/class) [49], Cars-196 (~40 img/class) [22] and Food-101 (750 img/class) [5]. Table 1 shows
188 results for the two popular backbones ResNet-50 [15] and DenseNet-169 [17], exchanging the output
189 layer accordingly. In 53/56 settings, we see improved results over standard layers. Of these, 48
190 and 36 are significant with $p < 0.1$ and $p < 0.001$, respectively. Although there is no clear best
191 method, it is worth noting that sparse and ensemble layers as enhancements of both random and
192 1-to-1 layers are significantly better ($p < 0.001$) in 7/8 settings, respectively. As expected, smaller
193 performance differences are exhibited in Food-101, which is a considerably larger dataset, thus
194 requiring less regularization. Among the worse settings, only 1 is significant ($p < 0.1$) for Food-101
195 since it involves strong regularization to multiple layers. These regularizers are discussed separately
196 in Sect. 5.5.

197 5.2 Large-scale classification and transfer learning

198 Machine learning models are subject to the bias-variance tradeoff [12], in which induced biases of
199 the presented output layers might be too strong to fit the training data. We therefore want to shed
200 light on how these layers behave in large-scale and transfer learning settings, where overfitting is
201 less problematic. Datasets include CIFAR-100 (C100, 5000 img/class) [23], ImageNet (IN, ~1200
202 img/class) from ILSVRC2012 [37] reported on the validation set, as well as CUB/Cars/Food with
203 models being pre-trained on IN. Table 2 shows the results for the ResNet-50 backbone. In C100,
204 we see consistent improvements with at least $p < 0.1$. On the other datasets, results are mostly
205 comparable corroborating widespread applicability. It is worth mentioning that W^{1to1} and $W^{ensemble}$
206 perform consistently better, and $W^{ensemble}$ significantly ($p < 0.1$) in multiple cases. With growing
207 dataset sizes, both layers expose a strong constraint on the class neurons to fit an increasing number
208 of examples. We believe this to be responsible for progressively separating the signal from the noise,
209 leading to better generalization. On the other hand, neuron dependency is reduced in larger datasets
210 (see Fig. 3 left) diminishing the effect of W^{scale} and W^{random} . Moreover, W^{random} and W^{sparse}
211 can be affected by predetermined feature-class weights that do not have to match features learned
212 during pre-training, which might require larger adjustments to the weights of the last conv layer.

Table 1: Classification accuracy for different output layer designs in small-scale and fine-grained classification without pre-training. Exponent repeats describe probability values (*: $p < 0.1$, **: $p < 0.01$, ***: $p < 0.001$) indicating statistical significance based on a one-tailed normal approximation interval test comparing accuracy of the proposed layer designs to a baseline fc layer ($W^{trained}$). Symbols * and † denote better/worse performance than baseline, respectively. **Bold** denotes best performance.

		STL-10	CUB-200	Cars-196	Food-101
ResNet-50	$W^{trained}$ (baseline)	81.36	57.18	81.20	83.70
	W^{scaled}	83.33*	63.46***	87.07***	85.46***
	W^{scaled} block	86.42***	66.74***	87.53***	85.03**
	W^{random}	86.08***	60.91**	83.02*	84.20
	W^{random} block	86.59***	67.21***	84.07***	84.04
	W^{sparse}	87.23***	66.27***	85.47***	85.45***
	W^{1to1}	84.78***	58.56	80.51	84.41*
	$W^{ensemble}$	87.94***	62.98***	85.76***	85.36***
DenseNet-169	$W^{trained}$ (baseline)	81.88	55.33	80.82	84.31
	W^{scaled}	86.53***	63.31***	85.85***	85.05*
	W^{scaled} block	85.89***	65.57***	85.35***	85.44**
	W^{random}	86.11***	61.24***	83.52**	84.90*
	W^{random} block	86.64***	65.99***	82.93*	83.25†
	W^{sparse}	86.58***	62.75***	85.79***	84.63
	W^{1to1}	86.06***	55.37	83.75**	84.11
	$W^{ensemble}$	87.00***	64.15***	85.09***	84.91*

Table 2: Classification results for different output layer designs in large-scale image recognition and transfer learning. + denotes fine-tuning from ImageNet. See Table 1 for other symbols.

	C100	IN-top1	IN-top5	CUB-200+	Cars-196+	Food-101+
$W^{trained}$	77.75	76.36	93.12	80.91	91.73	87.32
W^{scaled}	79.65*	76.08	92.84	78.68†	90.91†	87.21
W^{random}	78.91*	76.08	93.15	80.89	91.72	87.29
W^{sparse}	79.46*	75.32††	92.36†††	80.38	92.07	87.31
W^{1to1}	79.07*	76.53	93.32	81.79	91.87	87.31
$W^{ensemble}$	80.38***	76.62	93.46*	82.22*	92.77*	87.76

213 5.3 Use Case: Medical imaging

214 Output layer design is critical in fields such as medical imaging, which presents special challenges to
 215 regularization: Datasets tend to be small, imbalanced, abnormalities might fill only a few pixels of
 216 the image, and appearances between classes are often similar. In addition, transfer learning with IN
 217 weights is either inaccessible due to architectural differences (e.g. image segmentation, 3D Magnetic
 218 Resonance Imaging) or less effective due to large domain differences. This is first illustrated on the
 219 APTOS Kaggle challenge dataset (3662 images, 193-1805 img/class) [20], with the goal of detecting
 220 diabetic retinopathy severities in retinal fundus images. We use the public training dataset to train a
 221 multi-class classifier and perform 5-fold cross-validation. Table 3 shows the results. We consistently
 222 get better performance with regularization and reduce the gap to a pre-trained network. Furthermore,
 223 an additional experiment in the appendix indicates that the standard output layer is biased towards the
 224 prevalent class, which is inherently remedied through randomization.

225 We provide further evidence that the proposed layer designs positively affect tasks other than
 226 classification. We learn a U-Net [35] for binary semantic slice-based segmentation of Computed
 227 Tomography scans of livers comparing a standard 1x1 conv output layer with 64 parameters to both a
 228 fixed randomized and an ensemble layer. Due to the limited number of parameters, we omit W^{scale}
 229 and W^{sparse} here. Different to classification, the output of a U-Net itself can be interpreted as a 1-to-1
 230 layer. One can still build an ensemble by treating each output channel as a head. Both W^{random} and
 231 $W^{ensemble}$ ($H = 10$) are then applied to the CHAOS [21] and SLIVER [47] datasets. For CHAOS,

Table 3: Quadratic weighted kappa and accuracy (with significance) for different output layers in ResNet-50 for the APTOS dataset. + denotes fine-tuning from IN. See Table 1 for other symbols.

	Kappa	Acc.
$W^{trained}$	0.816	77.44
W^{scaled}	0.818	78.38
W^{random}	0.848	79.32*
W^{sparse}	0.840	79.60*
W^{1to1}	0.856	80.08*
$W^{ensemble}$	0.866	80.78**
$W^{trained+}$	0.909	85.02
$W^{sparse+}$	0.910	85.17
$W^{ensemble+}$	0.912	85.56

Table 4: Jaccard coefficients in segmentation

	CHAOS	SLIVER
$W^{trained}$	0.77	0.83
W^{random}	0.80	0.85
$W^{ensemble}$	0.78	0.86

Table 5: Regularization comparison

	STL	CUB	CUB+	Cars
Dropout [42]	82.73	63.20	80.26	83.98
Dropconn. [50]	86.15	61.48	80.41	85.06
Add. Noise [10]	82.51	52.74	80.91	76.77
$W^{trained}$	81.36	57.18	80.91	81.20
W^{sparse}	87.23	66.27	80.38	85.47
$W^{ensemble}$	87.94	62.98	82.22	85.76

232 we train on 15 randomly selected patients (2155 slices) and evaluate on the remaining 5 (719 slices).
 233 We then test for generalization by training on all 20 patients from CHAOS and evaluating on the
 234 external SLIVER dataset consisting of 20 patients (4159 slices). Table 4 shows improved results in
 235 both settings.

236 5.4 Other regularization techniques

237 Table 5 compares our most competitive methods to other popular regularizers when applied to a
 238 standard output layer. Nodes/connections in dropout/dropconnect are both removed with $p = 0.7$,
 239 and the noise layer adds a Gaussian with $\mu = 0$ and $\sigma = 0.1$ before applying the fc layer. In all
 240 cases, our variants perform better. Whereas noise does not benefit training here, dropout/-connect is
 241 supporting regularization. However, both of the latter methods come with two main disadvantages.
 242 First, they add complexity by changing states in each iteration and having different behavior during
 243 training and inference. Second, hyperparameter tuning is necessary, while our layers are either
 244 hyperparameter-free or stable to them. See the ablation study in Sect. 5.7 for evidence.

245 5.5 Beyond output layers - block scaling and randomization

246 Activation scaling and randomization are techniques applicable to any layer and increase regulariza-
 247 tion further. This is demonstrated for ResNet-50 and DenseNet-169 in Table 1. Both architectures
 248 consist of multiple blocks, each holding groups of conv layer, batch normalization (BN) and activa-
 249 tion function. For W^{random} block, all layers of the last block and the output layer are kept in their
 250 initialized state during training. Similarly, in W^{scaled} block, activations of all layer groups in the last
 251 block are scaled during training. In ResNet-50, block scaling outperforms output layer scaling in 3/4
 252 datasets by up to 3% points, and block randomization increases performance in 3/4 datasets by up to
 253 6% points compared to output layer randomization. In DenseNet-169, block scaling outperforms out-
 254 put layer scaling in 2/4 datasets by up to 2% points, and block randomization increases performance
 255 in 2/4 datasets by up to 4% points compared to output layer randomization. Only in Food-101 and
 256 DenseNet, block randomization performs significantly worse than baseline because regularization is
 257 too strong leading to underfitting ($train\ loss = 0.47$ compared to 0.02 in W^{random}).

258 5.6 Computational efficiency

259 The design of the head of deep CNNs has a great impact on computational efficiency. Standard output
 260 layers alone can contain a large amount of parameters, as CNNs typically hold more channels as
 261 they get deeper and the number of classes can become large. In ImageNet and a ResNet-50, for
 262 example, the output layer alone generates over 2 million parameters, which are saved in W^{1to1} and
 263 $W^{ensemble}$. This problem compounds when using multiple fc layers. In a VGG-16, for instance, 3 fc
 264 layers are employed after the last conv layer. As Table 6 shows, omitting all fc layers saves up to
 265 90% in parameters, a considerable amount of memory, and time for a forward/backward pass while

Table 6: Computational efficiency comparison in CUB-200 highlighting that the number of trainable parameters can often be reduced while accuracy is improved. + denotes fine-tuning from ImageNet.

Architecture	#Params in M.	Mem.[GB]	GFLOPS	Time [ms/it.]	Accuracy
VGG16 $W^{trained+}$	135.1	7.5	31.1	114	78.68
VGG16 W^{1to1+}	13.5	5.9	30.4	106	79.27
VGG16 $W^{ensemble+}$	14.7	5.9	30.8	106	81.15**
Res50 $W^{trained}$	23.9	5.1	8.2	71	57.18
Res50 W^{random} block	8.5	5.0	8.2	67	67.21***

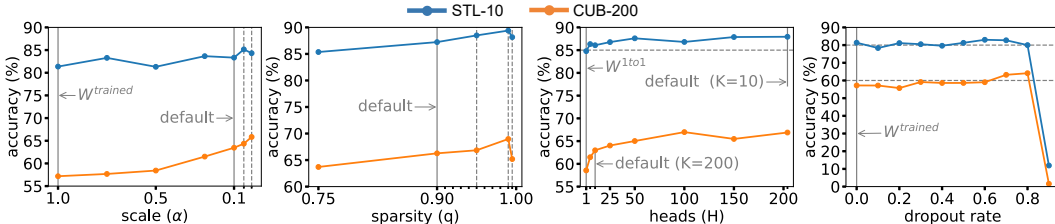


Figure 6: Ablation study showing stability and consistency of our output layer designs

266 increasing accuracy. If a ResNet-50 is used, randomization of the last conv block next to the output
 267 layer yields savings of about 65% in trainable parameters while increasing accuracy by 10% points.

268 5.7 Ablation study

269 Note that W^{random} and W^{1to1} are hyperparameter-free compared to other regularizers such as
 270 dropout/-connect, thus saving the cost of tuning them. Although other layer variants possess hyperpa-
 271 rameters, we show in Fig. 6 for the ResNet backbone that they are stable (no large jumps in vicinity)
 272 and consistent (tend to monotonicity w.r.t. performance). In W^{sparse} , the maximum accuracy for
 273 both datasets is at $q = 0.99$ (20 nodes per class) and drops only slightly for $q = 0.995$. Similarly,
 274 downscaling in W^{scale} improves performance at a small cost if the optimum is not hit. Also, more
 275 heads in $W^{ensemble}$ tend to increase performance. What is the result of adding more heads than
 276 given by the constraint $N = KH$? If $N < KH$, which is the case for CUB-200 and $H > 10$, we
 277 add an additional 1×1 conv layer, BN and ReLU with KH nodes to adjust for the missing channels.
 278 Although this leads to a considerable increase in parameters (NKH for the conv layer), it helps with
 279 generalization, contradicting the common belief that overparameterization leads to overfitting [48].
 280 In contrast, dropout is not stable or consistent. With a dropout rate of 0.9, the network fails to train
 281 in both datasets. Furthermore, the optimum for CUB lies at 0.8, the same hyperparameter choice in
 282 STL would result in worse performance than baseline.

283 6 Conclusion

284 In this work, we introduced neuron dependency and expressivity as factors contributing to overfitting.
 285 Then, different output layers were defined to optimize both and showed improved regularization in
 286 various settings while being efficient and robust to hyperparameters. Although these layers are simple,
 287 they have high practical relevance due to the importance of regularization and the ubiquity of output
 288 layers in deep nets. In addition to their application, they may also be useful as primitives in future
 289 (automatically created) architectures. Although improving regularization, we note that optimizing
 290 for neuron dependencies/expressivity does not *solve* overfitting. For example, an unknown or noisy
 291 instance may result in reduced activations in the majority of nodes in the penultimate layer. Finally,
 292 we speculate that overfitting may not just be a function of the number of parameters in the encoder.
 293 Instead, it might be more important how the extracted features are combined in the output layer.

294 **References**

- 295 [1] Antreas Antoniou, Amos Storkey, and Harrison Edwards. Data augmentation generative
296 adversarial networks. *arXiv preprint arXiv:1711.04340*, 2017.
- 297 [2] Devansh Arpit, Stanisław Jastrzębski, Nicolas Ballas, David Krueger, Emmanuel Bengio,
298 Maxinder S Kanwal, Tegan Maharaj, Asja Fischer, Aaron Courville, Yoshua Bengio, et al.
299 A closer look at memorization in deep networks. In *International Conference on Machine*
300 *Learning*, pages 233–242. PMLR, 2017.
- 301 [3] Jimmy Lei Ba, Jamie Ryan Kiros, and Geoffrey E Hinton. Layer normalization. *arXiv preprint*
302 *arXiv:1607.06450*, 2016.
- 303 [4] David Baehrens, Timon Schroeter, Stefan Harmeling, Motoaki Kawanabe, Katja Hansen, and
304 Klaus-Robert Müller. How to explain individual classification decisions. *The Journal of*
305 *Machine Learning Research*, 11:1803–1831, 2010.
- 306 [5] Lukas Bossard, Matthieu Guillaumin, and Luc Van Gool. Food-101 – mining discriminative
307 components with random forests. In *European Conference on Computer Vision*, 2014.
- 308 [6] Rich Caruana. Multitask learning. *Machine learning*, 28(1):41–75, 1997.
- 309 [7] Rich Caruana, Steve Lawrence, and Lee Giles. Overfitting in neural nets: Backpropagation,
310 conjugate gradient, and early stopping. *Advances in neural information processing systems*,
311 pages 402–408, 2001.
- 312 [8] Soravit Changpinyo, Mark Sandler, and Andrey Zhmoginov. The power of sparsity in convolu-
313 tional neural networks. *arXiv preprint arXiv:1702.06257*, 2017.
- 314 [9] Adam Coates, Andrew Ng, and Honglak Lee. An analysis of single-layer networks in unsuper-
315 vised feature learning. In *Proceedings of the fourteenth international conference on artificial*
316 *intelligence and statistics*, pages 215–223. JMLR Workshop and Conference Proceedings, 2011.
- 317 [10] Terrance DeVries and Graham W Taylor. Dataset augmentation in feature space. *arXiv preprint*
318 *arXiv:1702.05538*, 2017.
- 319 [11] Jonathan Frankle and Michael Carbin. The lottery ticket hypothesis: Finding sparse, trainable
320 neural networks. *arXiv preprint arXiv:1803.03635*, 2018.
- 321 [12] Stuart Geman, Elie Bienenstock, and René Doursat. Neural networks and the bias/variance
322 dilemma. *Neural computation*, 4(1):1–58, 1992.
- 323 [13] Xavier Glorot, Antoine Bordes, and Yoshua Bengio. Deep sparse rectifier neural networks. In
324 *Proceedings of the fourteenth international conference on artificial intelligence and statistics*,
325 pages 315–323. JMLR Workshop and Conference Proceedings, 2011.
- 326 [14] Moritz Hardt and Tengyu Ma. Identity matters in deep learning. *arXiv preprint*
327 *arXiv:1611.04231*, 2016.
- 328 [15] Kaiming He, Xiangyu Zhang, Shaoqing Ren, and Jian Sun. Deep residual learning for image
329 recognition. In *Proceedings of the IEEE conference on computer vision and pattern recognition*,
330 pages 770–778, 2016.
- 331 [16] Elad Hoffer, Itay Hubara, and Daniel Soudry. Fix your classifier: the marginal value of training
332 the last weight layer. *arXiv preprint arXiv:1801.04540*, 2018.
- 333 [17] Gao Huang, Zhuang Liu, Laurens Van Der Maaten, and Kilian Q Weinberger. Densely connected
334 convolutional networks. In *Proceedings of the IEEE conference on computer vision and pattern*
335 *recognition*, pages 4700–4708, 2017.
- 336 [18] Guang-Bin Huang, Qin-Yu Zhu, and Chee-Kheong Siew. Extreme learning machine: theory
337 and applications. *Neurocomputing*, 70(1-3):489–501, 2006.
- 338 [19] Sergey Ioffe and Christian Szegedy. Batch normalization: Accelerating deep network training
339 by reducing internal covariate shift. In *International conference on machine learning*, pages
340 448–456. PMLR, 2015.

- 341 [20] Kaggle. Aptos 2019 blindness detection, 2019. URL [https://www.kaggle.com/c/](https://www.kaggle.com/c/aptos2019-blindness-detection)
342 [aptos2019-blindness-detection](https://www.kaggle.com/c/aptos2019-blindness-detection).
- 343 [21] A Emre Kavur, N Sinem Gezer, Mustafa Barış, Sinem Aslan, Pierre-Henri Conze, Vladimir
344 Groza, Duc Duy Pham, Soumick Chatterjee, Philipp Ernst, Savaş Özkan, et al. Chaos challenge-
345 combined (ct-mr) healthy abdominal organ segmentation. *Medical Image Analysis*, 69:101950,
346 2021.
- 347 [22] Jonathan Krause, Michael Stark, Jia Deng, and Li Fei-Fei. 3d object representations for
348 fine-grained categorization. In *4th International IEEE Workshop on 3D Representation and*
349 *Recognition (3dRR-13)*, Sydney, Australia, 2013.
- 350 [23] Alex Krizhevsky, Geoffrey Hinton, et al. Learning multiple layers of features from tiny images.
351 2009.
- 352 [24] Alex Krizhevsky, Ilya Sutskever, and Geoffrey E Hinton. Imagenet classification with deep
353 convolutional neural networks. *Advances in neural information processing systems*, 25:1097–
354 1105, 2012.
- 355 [25] Jan Kukačka, Vladimir Golkov, and Daniel Cremers. Regularization for deep learning: A
356 taxonomy. *arXiv preprint arXiv:1710.10686*, 2017.
- 357 [26] Yann A LeCun, Léon Bottou, Genevieve B Orr, and Klaus-Robert Müller. Efficient backprop.
358 In *Neural networks: Tricks of the trade*, pages 9–48. Springer, 2012.
- 359 [27] Namhoon Lee, Thalaiyasingam Ajanthan, and Philip HS Torr. Snip: Single-shot network
360 pruning based on connection sensitivity. *arXiv preprint arXiv:1810.02340*, 2018.
- 361 [28] Min Lin, Qiang Chen, and Shuicheng Yan. Network in network. *arXiv preprint arXiv:1312.4400*,
362 2013.
- 363 [29] Baoyuan Liu, Min Wang, Hassan Foroosh, Marshall Tappen, and Marianna Pinsky. Sparse
364 convolutional neural networks. In *Proceedings of the IEEE conference on computer vision and*
365 *pattern recognition*, pages 806–814, 2015.
- 366 [30] Eran Malach, Gilad Yehudai, Shai Shalev-Schwartz, and Ohad Shamir. Proving the lottery
367 ticket hypothesis: Pruning is all you need. In *International Conference on Machine Learning*,
368 pages 6682–6691. PMLR, 2020.
- 369 [31] Federico Pernici, Matteo Bruni, Claudio Baccchi, and Alberto Del Bimbo. Fix your features:
370 Stationary and maximally discriminative embeddings using regular polytope (fixed classifier)
371 networks. *arXiv preprint arXiv:1902.10441*, 2019.
- 372 [32] David C Plaut, Steven J Nowlan, and Geoffrey E Hinton. Experiments on learning by back
373 propagation. 1986.
- 374 [33] Zhongchao Qian. *Deep Convolutional Networks without Learning the Classifier Layer*. PhD
375 thesis, Rochester Institute of Technology, 2020.
- 376 [34] Prajit Ramachandran, Niki Parmar, Ashish Vaswani, Irwan Bello, Anselm Levskaya, and
377 Jonathon Shlens. Stand-alone self-attention in vision models. *arXiv preprint arXiv:1906.05909*,
378 2019.
- 379 [35] Olaf Ronneberger, Philipp Fischer, and Thomas Brox. U-net: Convolutional networks for
380 biomedical image segmentation. In *International Conference on Medical image computing and*
381 *computer-assisted intervention*, pages 234–241. Springer, 2015.
- 382 [36] Amir Rosenfeld and John K Tsotsos. Intriguing properties of randomly weighted networks:
383 Generalizing while learning next to nothing. In *2019 16th Conference on Computer and Robot*
384 *Vision (CRV)*, pages 9–16. IEEE, 2019.
- 385 [37] Olga Russakovsky, Jia Deng, Hao Su, Jonathan Krause, Sanjeev Satheesh, Sean Ma, Zhiheng
386 Huang, Andrej Karpathy, Aditya Khosla, Michael Bernstein, Alexander C. Berg, and Li Fei-Fei.
387 ImageNet Large Scale Visual Recognition Challenge. *International Journal of Computer Vision*
388 *(IJCV)*, 115(3):211–252, 2015. doi: 10.1007/s11263-015-0816-y.

- 389 [38] Holger Schwenk and Yoshua Bengio. Boosting neural networks. *Neural computation*, 12(8):
390 1869–1887, 2000.
- 391 [39] Gabi Shalev, Gal-Lev Shalev, and Joseph Keshet. Redesigning the classification layer by
392 randomizing the class representation vectors. *arXiv preprint arXiv:2011.08704*, 2020.
- 393 [40] Connor Shorten and Taghi M Khoshgoftaar. A survey on image data augmentation for deep
394 learning. *Journal of Big Data*, 6(1):1–48, 2019.
- 395 [41] Jost Tobias Springenberg, Alexey Dosovitskiy, Thomas Brox, and Martin Riedmiller. Striving
396 for simplicity: The all convolutional net. *arXiv preprint arXiv:1412.6806*, 2014.
- 397 [42] Nitish Srivastava, Geoffrey Hinton, Alex Krizhevsky, Ilya Sutskever, and Ruslan Salakhutdinov.
398 Dropout: a simple way to prevent neural networks from overfitting. *The journal of machine*
399 *learning research*, 15(1):1929–1958, 2014.
- 400 [43] Christian Szegedy, Wei Liu, Yangqing Jia, Pierre Sermanet, Scott Reed, Dragomir Anguelov,
401 Dumitru Erhan, Vincent Vanhoucke, and Andrew Rabinovich. Going deeper with convolutions.
402 In *Proceedings of the IEEE conference on computer vision and pattern recognition*, pages 1–9,
403 2015.
- 404 [44] Mingxing Tan and Quoc Le. Efficientnet: Rethinking model scaling for convolutional neural
405 networks. In *International Conference on Machine Learning*, pages 6105–6114. PMLR, 2019.
- 406 [45] Hidenori Tanaka, Daniel Kunin, Daniel LK Yamins, and Surya Ganguli. Pruning neural networks
407 without any data by iteratively conserving synaptic flow. *arXiv preprint arXiv:2006.05467*,
408 2020.
- 409 [46] Robert Tibshirani. Regression shrinkage and selection via the lasso. *Journal of the Royal*
410 *Statistical Society: Series B (Methodological)*, 58(1):267–288, 1996.
- 411 [47] Bram Van Ginneken, Tobias Heimann, and Martin Styner. 3d segmentation in the clinic: A
412 grand challenge. In *MICCAI Workshop on 3D Segmentation in the Clinic: A Grand Challenge*,
413 volume 1, pages 7–15, 2007.
- 414 [48] N Vapnik Vladimir and V Vapnik. Statistical learning theory. *Xu JH and Zhang XG. translation.*
415 *Beijing: Publishing House of Electronics Industry, 2004*, 1998.
- 416 [49] C. Wah, S. Branson, P. Welinder, P. Perona, and S. Belongie. The Caltech-UCSD Birds-200-2011
417 Dataset. Technical Report CNS-TR-2011-001, California Institute of Technology, 2011.
- 418 [50] Li Wan, Matthew Zeiler, Sixin Zhang, Yann Le Cun, and Rob Fergus. Regularization of
419 neural networks using dropconnect. In *International conference on machine learning*, pages
420 1058–1066. PMLR, 2013.
- 421 [51] Chaoqi Wang, Guodong Zhang, and Roger Grosse. Picking winning tickets before training by
422 preserving gradient flow. *arXiv preprint arXiv:2002.07376*, 2020.
- 423 [52] Chiyuan Zhang, Samy Bengio, Moritz Hardt, Benjamin Recht, and Oriol Vinyals. Understanding
424 deep learning requires rethinking generalization. *arXiv preprint arXiv:1611.03530*, 2016.
- 425 [53] Chiyuan Zhang, Samy Bengio, Moritz Hardt, Michael C Mozer, and Yoram Singer. Identity
426 crisis: Memorization and generalization under extreme overparameterization. *arXiv preprint*
427 *arXiv:1902.04698*, 2019.

428 **Checklist**

- 429 1. For all authors...
- 430 (a) Do the main claims made in the abstract and introduction accurately reflect the paper’s
431 contributions and scope? [Yes] See Sect. 3, 5 and the appendix.
- 432 (b) Did you describe the limitations of your work? [Yes] See Sect. 4.5 ($N = K$ con-
433 straint), Sect. 5.2 (some layers are not optimal for large-scale datasets and fine-tuning),
434 Sect. 5.5 (strong regularization may lead to underfitting), and Sect. 6 (neuron depen-
435 dency/expressivity are factors of overfitting, but this does not constitute all factors).
- 436 (c) Did you discuss any potential negative societal impacts of your work? [N/A] Focus
437 is on architecture and technical, no particular application affecting society is targeted.
438 Note that medical ML applications should be thoroughly evaluated, e.g., for bias and
439 generalizability, before being used in practice.
- 440 (d) Have you read the ethics review guidelines and ensured that your paper conforms to
441 them? [Yes]
- 442 2. If you are including theoretical results...
- 443 (a) Did you state the full set of assumptions of all theoretical results? [N/A] Only empirical
444 results are included.
- 445 (b) Did you include complete proofs of all theoretical results? [N/A] Only empirical results
446 are included.
- 447 3. If you ran experiments...
- 448 (a) Did you include the code, data, and instructions needed to reproduce the main ex-
449 perimental results (either in the supplemental material or as a URL)? [Yes] Code
450 implementing the shown layer types and dataset descriptions are given in the supple-
451 mental material/appendix.
- 452 (b) Did you specify all the training details (e.g., data splits, hyperparameters, how they
453 were chosen)? [Yes] We report the corresponding splits if not defined by the datasets
454 themselves. Hyperparameters and information about the training are partly provided in
455 the main text (e.g. architecture type, layer hyperparameters) and are detailed further in
456 the appendix.
- 457 (c) Did you report error bars (e.g., with respect to the random seed after running experi-
458 ments multiple times)? [Yes] We indicate statistical significance for our classification
459 results.
- 460 (d) Did you include the total amount of compute and the type of resources used (e.g., type
461 of GPUs, internal cluster, or cloud provider)? [Yes] We have not tracked CO2 due to
462 missing awareness but some details about the setup are provided in the appendix. We
463 plan to track CO2 in subsequent works.
- 464 4. If you are using existing assets (e.g., code, data, models) or curating/releasing new assets...
- 465 (a) If your work uses existing assets, did you cite the creators? [Yes] See Sect. 5. This is
466 done after first mentioning the corresponding datasets in the main text.
- 467 (b) Did you mention the license of the assets? [Yes] We mention asset licenses in the
468 appendix.
- 469 (c) Did you include any new assets either in the supplemental material or as a URL? [Yes]
470 We provide code as supplemental material.
- 471 (d) Did you discuss whether and how consent was obtained from people whose data you’re
472 using/curating? [N/A] The datasets in Sect. 5.3 are open source from past challenges
473 and contain de-identified data to the best of our knowledge. Further details on data
474 collection are provided in the corresponding references.
- 475 (e) Did you discuss whether the data you are using/curating contains personally identi-
476 fiable information or offensive content? [N/A] All datasets are commonly used for
477 benchmarks and/or do not contain obviously offensive content. However, ImageNet
478 likely contains images showing persons.
- 479 5. If you used crowdsourcing or conducted research with human subjects...

- 480 (a) Did you include the full text of instructions given to participants and screenshots,
481 if applicable? [N/A] No crowdsourcing or research with human subjects has been
482 conducted.
- 483 (b) Did you describe any potential participant risks, with links to Institutional Review
484 Board (IRB) approvals, if applicable? [N/A] See above.
- 485 (c) Did you include the estimated hourly wage paid to participants and the total amount
486 spent on participant compensation? [N/A] See above.